Influence of Ion Mass on Electrical Elements of an Ion Sheath: A Comparative Study

Mrinal Kumar Mishra
[1]Department of Physics, Baosi.Banikanta.Kakati.College, Nagaon, Barpeta,
Assam-781311, India.
e-mail: mishra.mrinal@rediffmail.com

Abstract: The effect of ion mass on the values of electrical elements such as capacitance (C), resistance (R) and inductance (L) for a D.C ion sheath has been theoretically examined. Quantitative estimations of the L, C and R components as a function of plasma density and sheath potential are analyzed for atomic argon and molecular nitrogen plasma at a particular electron temperature. Values of calculated frequencies are found to be higher for gas with lower atomic mass. It is seen that values of inductance and resistance are highly dependent on ion mass, whereas values of capacitance is mass independent. Further the values of inductance and resistance are found to be higher for higher atomic mass.

Keywords: Ion sheath, Ion transit time, Ion plasma frequency.

1. Introduction:

Sheath formation at the plasma boundary is a unique problem in plasma physics and has been receiving importance because plasma sheath interaction physics have various roles to play in fundamental research of confined plasmas [1-3].

The sheath, which is an interface between the solid and the plasma, mediates the flow of particles and energy out of the plasma to the solid surface [4,5]. The basic properties of the plasma, such as its density and temperature, often strongly dependent on the way solid and plasma interact. At the interface between the solid and the plasma, a thin net-charge layer called the Debye sheath develops spontaneously.

In case of two-component and non-isothermal bounded plasma (T_e>>T_i) system, the electrons, being far mobile than the ions due to combined effects of their differential temperatures and inertial (mass) qualities, are rapidly lost to the boundary wall. Due to the higher thermal motions of the electrons, the boundary surface of the plane electrode/ or wall receives more thermal flux of electrons than that of the ions. Thus a net loss of thermal flux of the electrons from the bulk plasma occurs to the wall. As a result, the wall/ or electrode acquires negative potential with respect to whole bulk plasma that becomes a reservoir of excess positive ions. The typical scale size of the nonlinearly localized positive space charge dominated region, supposed to shield the negative wall potential comes out to be of the order of a few Debye lengths [6].

The sheath formation is a natural consequence of the boundary effect on plasma to provide a self-consistent confining potential barrier to prevent thermal loss of the highly mobile species like electrons in any normal two component plasmas.

If the sheath potential accelerates the ions towards the wall (negative biasing) and the wall draws mainly ion current, the resulting sheath is called as the "*ion rich sheath*". For significantly high negative voltage at the electrode, the electrode current is usually described by the Child-Langmuir law of space charge limited current and is accordingly called as "*Child-Langmuir sheath*"[7].

It is an established fact that the D.C positive ion rich sheath (in Child limit) is equivalent to a series electrical circuit consisting of resistance (R), inductance (L), and capacitance (C) as the circuit elements under the diode like ion sheath approximation in presence of low frequency oscillation but the oscillation frequency must be lower than the ion plasma frequency [8].
The physical origin of sheath capacitance could be the formation of localized positive space charge layer to shield the negative wall potential and origin of sheath resistance could be associated with the ions in motion, which have to overcome the potential barrier to pass through the positive space charge layer. The physical origin of sheath inductance is not clearly mentioned in literature, but it may be cause of some wavy motion of ions.
Earlier M.K.Mishra et al studied the variation of these electrical components as a function of plasma density in argon plasma [9]. The values of these sheath elements are estimated as a function of sheath potential has also been studied by Mishra and Ram-Prakash et al [10,11].
In the present work, we have theoretically estimated the frequency of oscillations for different density considering argon and nitrogen plasma at a constant electron temperature using the experimentally verified formula [12]. Values of calculated frequency at a fixed density and grid bias are found to be higher for gas with lower atomic mass. It is found that L and R are ion mass dependent, whereas C is mass independent. Further the values of L and R are found to be higher for higher atomic mass.

2. Theory and Estimation:
For the theoretical estimation of sheath components, we have used experimentally verified theoretical relation from the work of Popa and Schrittwieser [12].
They performed the experiment in a Double Plasma device. In a DP device, there are two multi-dipole magnetic cages separated by a stainless steel mesh grid. The plasma can be produced independently in both the chambers by hot filament discharge method. In the experiment of Popa and Schrittwieser, plasma was produced only in the source chamber and target chamber was used as collector. Plasma leaks through the negatively biased (V_G) separating grid from source into target chamber. The plasma in target chamber was mainly a diffusion plasma. The source chamber was at ground potential and target chamber was either positively or negatively biased with respect to ground. For physical visualization, the source and target chamber along with bias voltage applied to grid (V_G) and target chamber (V_T) are shown schematically in Fig 1(a). The plasma potential in the target chamber changes almost linearly with the applied bias (V_T) and that created a difference in plasma potential between source and target chamber, which was referred as bi-potential asymmetry. The asymmetric bi-potential structure produced in the system is also shown schematically in Fig 1(b).
When a positive space charge layer forms around the grid, low frequency instability was observed in the positively biased target chamber. The frequency of oscillation arises due to asymmetric potential structure between the two plasma chambers.
Poap and Schrittwieser experimentally verified the theoretical relation between ion bounce frequency (f), plasma density (n) and grid bias voltage (V_G). They derived the expression for ion bounce frequency (f), plasma density (n) and grid bias (V_G) at effective electron temperature of 2.9 eV in argon plasma as

$$f^2=1.2\times10^{-2}(n/V_G^{1/2})\text{-------------------------------}(1)$$

According to the experiment referred here, f is the frequency observed in the target (diffusion) chamber and n is the plasma density of source (discharge) chamber of DP-device.
Similarly, if we consider nitrogen plasma (atomic mass 14) instead of argon plasma (atomic mass 40) at the same electron temperature, then the equation (1) takes the form as,

$$f^2=3.4\times10^{-2}(n/V_G^{1/2})\text{-------------------------------}(2)$$

The detail derivation of the above equation is available in reference [12]. In deriving equation (1) and (2), electron temperature is assumed to be constant and presence of impurity in the system is neglected.
Again, the electrical components of an ion sheath derived by Rosa are based on the solution of the Poisson's equation under collision less Child sheath approximation for low frequency fluctuations [8].
The expression of capacitance, inductance and resistance as derived by Rosa are as follows,

$R_{sh} = (c_s \tau^2_{io} \lambda^2/12\varepsilon_0)$------------------------(3)

$C_{sh} = (1+ \lambda^2/6)\ (\varepsilon_0/\chi_0)$--------------------(4)

$L_{sh} = -(c_s \tau^3_{io} \lambda^2/40\varepsilon_0)$----------------------(5)

Here, ε_0 is the vacuum permitivity, c_s is the ion acoustic speed, $\lambda=\omega_{pi}\ \tau_{io}$, where ω_{pi} is the ion plasma oscillation frequency and τ_{io} is the ion transit time through the sheath.
The equilibrium sheath width χ_0 (here denoted by d) is expressed in terms of ion transit time τ_{io} and ion acoustic speed c_s as

$\chi_0 = d = (1+\lambda^2/6)\ c_s \tau_{io}$ --------------------------(6)

We have used equation (1) to estimate the frequency of oscillations for different density for Argon plasma at a constant grid bias V_G=-140V. The ion transit time through sheath is approximated by the inverse of frequency of oscillation [13, 14]

$f = t_{io}^{-1}$-------------------------------------(7)

The frequencies of oscillation *(f),* ion plasma frequency $(\omega_{ip}=2\pi f_{ip})$, ion transit time (τ_{io}), λ^2, which are calculated for some arbitrary density of the order of $10^{14}/m^3$ in Argon plasma at constant electron temperature of 2.9 eV are shown in table 1.

Table. 1 : The frequency of oscillation (f), ion plasma frequency (ω_{ip}), ion transit time (τ_{io}), λ^2, calculated for different density for Argon plasma at V_G= -140V. The effective electron temperature 2.9 eV is considered.

Plasma density $n\ (10^{14} m^{-3})$	f (kHz)	τ_{io} (μs)	ω_{pi} (MHz)	C_S ($10^3 m/s$)	χ_0 (cm)	f/f_{ip}	λ
1	318	3.14	2.08	2.6	6.6	0.96	6.5
2	450	2.22	2.94		4.6	0.96	6.5
3	551	1.81	3.6		3.8	0.96	6.5
4	636	1.57	4.16		3.3	0.96	6.5

Similarly, in table 2, the frequencies of oscillation *(f),* ion plasma frequency $(\omega_{ip}=2\pi f_{ip})$, ion transit time (τ_{io}), λ^2, which are calculated for different density in Nitrogen plasma at constant electron temperature of 2.9 eV are shown.

Table. 2 : The frequency of oscillation (f), ion plasma frequency (ω_{ip}), ion transit time (τ_{io}), λ^2, calculated for different density for Nitrogen plasma at V_G= -140V. The effective electron temperature 2.9 eV is considered.

Plasma density n ($10^{14}m^{-3}$)	*f (kHz)*	τ_{io} *(μs)*	ω_{pi} *(MHz)*	C_S *(10^3m/s)*	χ_0 *(cm)*	f/f_{ip}	λ
1	536	1.86	3.51	4.4	6.6	0.96	6.5
2	758	1.31	4.97		4.6	0.96	6.5
3	928	1.07	6.09		3.8	0.96	6.5
4	1072	0.93	7.03		3.3	0.96	6.5

It is found that the estimated frequency of oscillation *f* increases with the increase in plasma density for a fixed grid bias voltage. The ratio f/f_{ip} (≈0.96) remains constant. The ratio f/f_{ip} <1 suggest that the frequency of oscillation is always less than the ion plasma frequency. In such a case, the ion current across the sheath is at all times in equilibrium with the applied voltage and is often assumed to obey Child's law for a space charge limited current.

The variation of estimated frequency of oscillation *f* with plasma density for argon and nitrogen plasma are shown in Fig. 3. The calculated frequency of oscillation is found to be higher for the gas with less atomic mass.

The sheath widths (χ_0, or *d*) obtained from relation (6) for different densities are plotted for two gases at a fixed grid bias voltage. This is shown in Fig.4. As usual, the sheath thickness found to contract with the increase in density and the sheath thickness remains almost the same for the two gases having different atomic mass.

The values of R_{sh} are calculated for different densities (frequency) using equation (3). The resistance decreases with the increase in plasma density and its value is higher for the heavier gas (having higher atomic mass). The variation of estimated sheath resistance with density is shown in Fig.5.

The sheath capacitances at different densities are estimated using equation (2). The sheath capacitance is found to increase with the increase in plasma density. The estimated values of sheath capacitance remains almost the same for the two gases. The variation of estimated sheath capacitance with density is shown in Fig.6.

The sheath inductance at different densities are estimated using equations (3).

The negative values of the sheath inductance are found to decreases with increase in plasma density. The sheath inductance posses higher negative value for the heavier gas. The variation of estimated sheath inductance with density is shown in Fig.7.

3. Conclusion:

The electrical components of an ion sheath are estimated by simple analytical approach from experimental parameters. We have used formulae found in literature to estimate these components as a function of argon and nitrogen plasma density.

In case of both resistance and inductance, the estimated values are found to be higher for heavier gas, i.e. mass dependent. In case of sheath capacitance, the values remain almost the same for both the gases, i.e. mass independent.

Reference:

[1] L.Tongs and I.Langmuir, Phys. Rev. 34, 876 (1929)
[2] K.U.Riemann, J.Phys.D:Appl.Phys, 24, 493, (1991)
[3] R.Choudura, Phys.Fluids, 25, 1628, (1982)
[4] M.K.Mishra, A.Phukan and M.Chakraborty, Chin.Phys.Lett 30, 015202, (2013)
[5] M.K.Mishra, A.Phukan , Chin.Phys.Lett 25, 1011, (2008)
[6] F.F.Chen, *"Introduction to Plasma Physics and Controlled Fusion"* (Plenum Press, New York, 1984) Vol.1
[7] C.K.Birdsall and W.B.Bridges, *"Electron Dynamics of Diode Regions,"* (Academic Press, New York, 1966)
[8] R.J.Rosa, J.Phys.A: Gen.Phys. 4, 934, (1971)
[9] M. K. Mishra et al Prog. Theor. Exp. Phys. **2014**, 033J01
[10] M. K. Mishra, Chin. J. Phys, 52, 1294 (2014)
[11] R. Prakash *et al* , Indian-J. Pure Appl. Phys, 40, 24, (2002)
[12] G.Popa and R.Schrittwieser, Phys.Plasmas 1, 32, (1994)
[13] A. Sarma, H. Bailung and J. Chutia, Phys. Plasmas 3, 3245, (1996)
[14] P.J.Barrett and G.R.Greaves, Phys.Fluids, B1,1776, (1989)

Figure Captions:

Fig. 1(a): Schematic diagram of a DP-device showing source chamber, target chamber and the grid. Presence of filament indicates that plasma is solely produced in source chamber. V_G and V_T are grid and target chamber bias respectively. I_G and I_T represents grid and target chamber current respectively.

Fig. 1(b): Schematic diagram shows the difference of plasma potential in source and target chamber caused by the target chamber bias V_T

Fig. 2: Schematic diagram of sheath equivalent series LCR circuit. L_{sh}, C_{sh}, R_{sh} and E denotes sheath associated inductance, capacitance, resistance and e.m.f respectively.

I denote Child current flowing through the circuit.

Fig. 3: The variation of the estimated frequency (f) at different plasma density (n) for argon and nitrogen plasma at fixed V_G= -140V.

Fig. 4: The variation of the estimated sheath thickness (d) at different plasma density (n) for argon and nitrogen plasma at fixed V_G= -140V.

Fig. 5: The variation of the estimated sheath resistance (R_{sh}) at different plasma density (n) for for argon and nitrogen plasma at fixed V_G= -140V.

Fig. 6: The variation of the estimated sheath capacitance (C_{sh}) at different plasma density (n) for argon and nitrogen plasma at fixed V_G= -140V.

Fig. 7: The variation of the estimated inductance (L_{sh}) at different plasma density for argon and nitrogen plasma at fixed V_G= -140V.

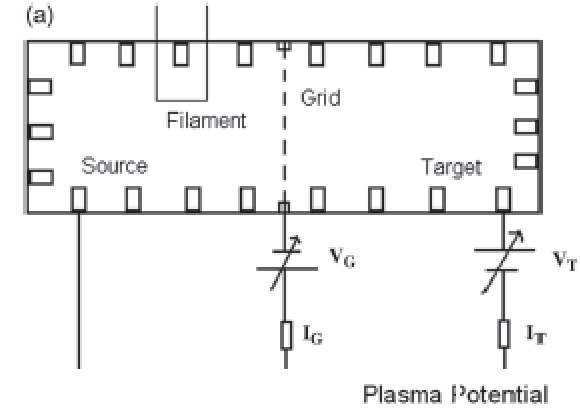

Fig.1 (a)

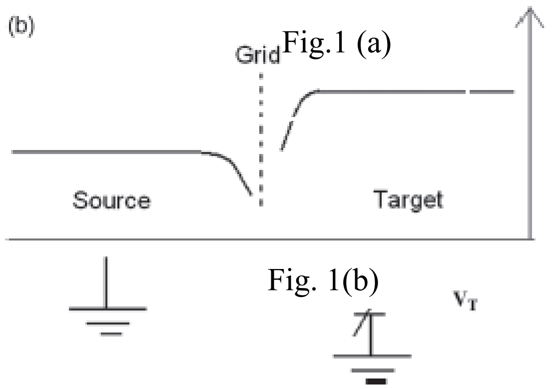

Fig. 1(b)

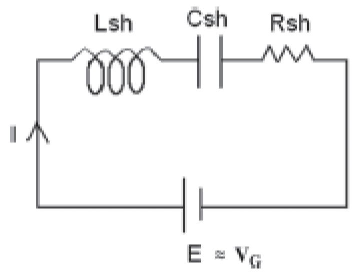

Fig. 2

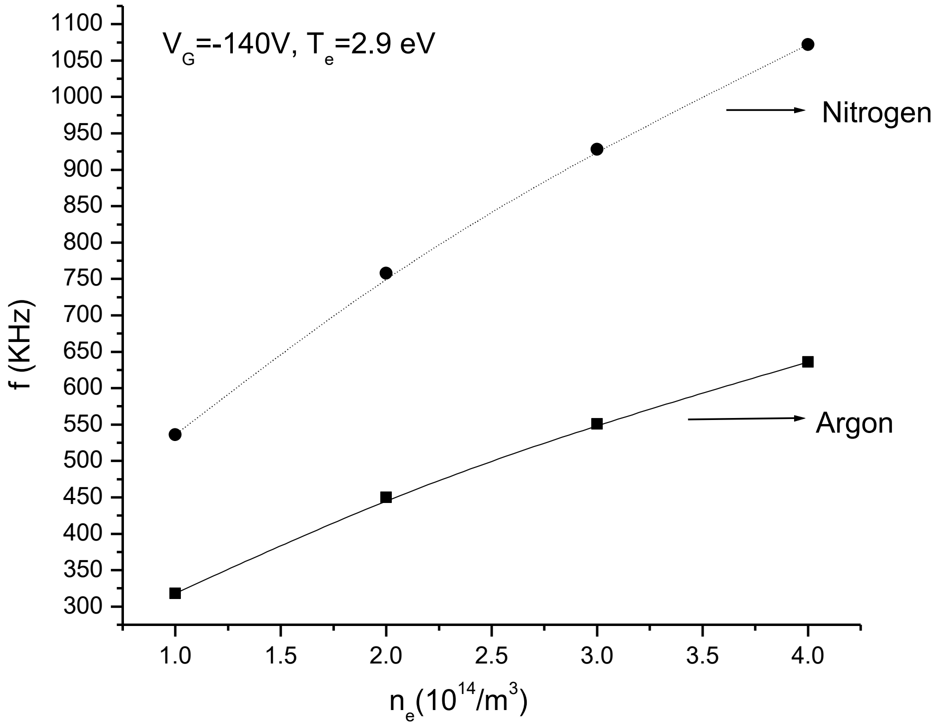
V_G=-140V, T_e=2.9 eV
Nitrogen
Argon
f (KHz)
$n_e(10^{14}/m^3)$

Fig.3

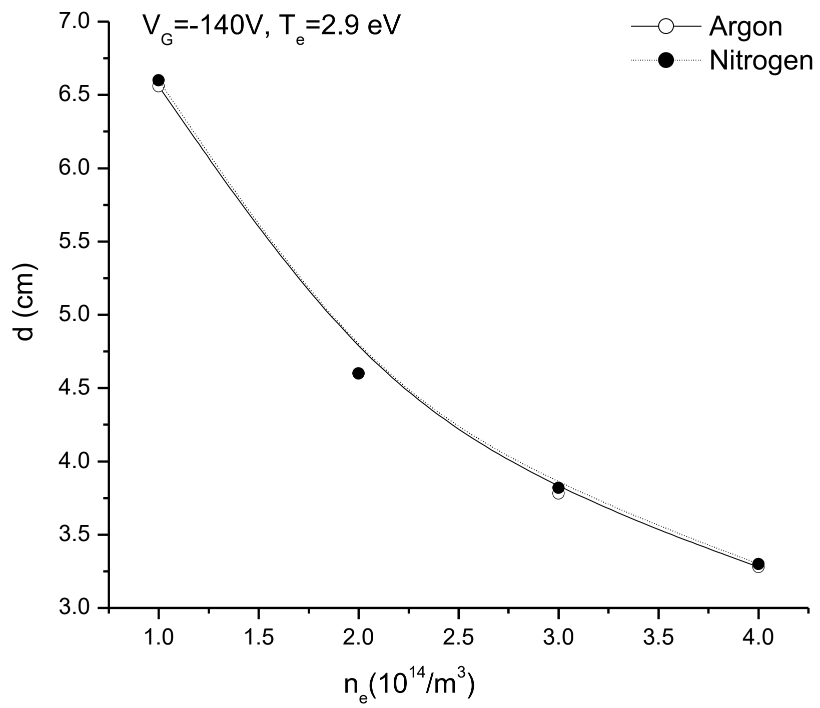
V_G=-140V, T_e=2.9 eV
Argon
Nitrogen
d (cm)
$n_e(10^{14}/m^3)$

Fig.4

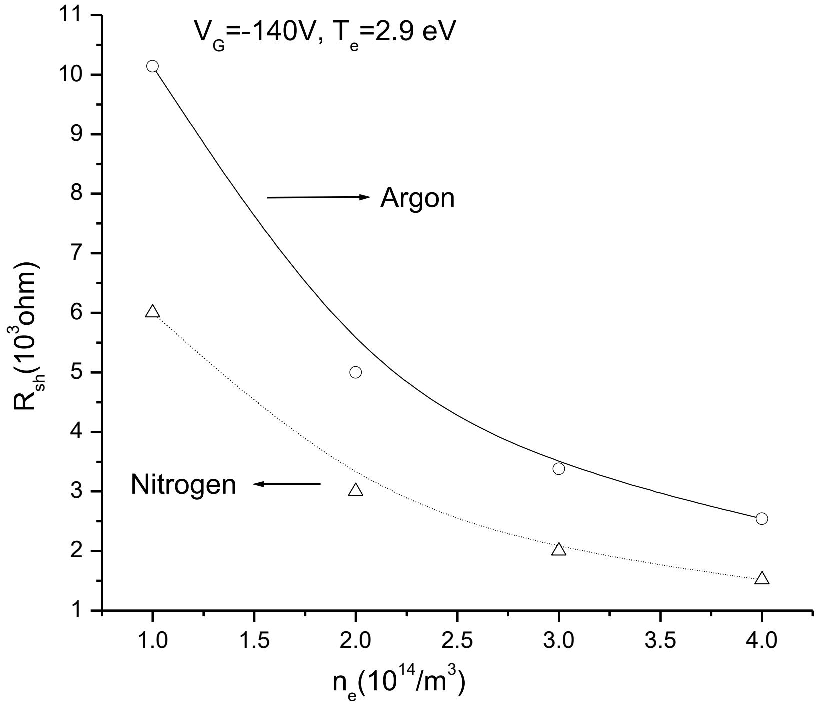
V_G=-140V, T_e=2.9 eV
Argon
Nitrogen
R_sh(10^3 ohm)
n_e(10^14/m^3)

Fig.5

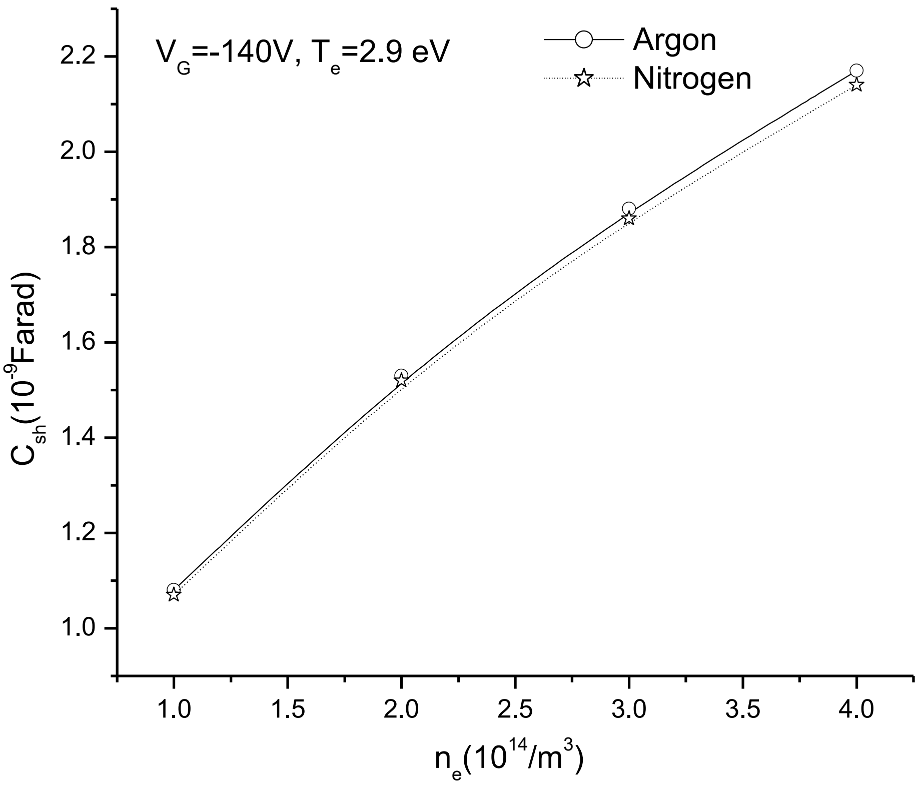
V_G=-140V, T_e=2.9 eV
Argon
Nitrogen
C_sh(10^-9 Farad)
n_e(10^14/m^3)

Fig.6

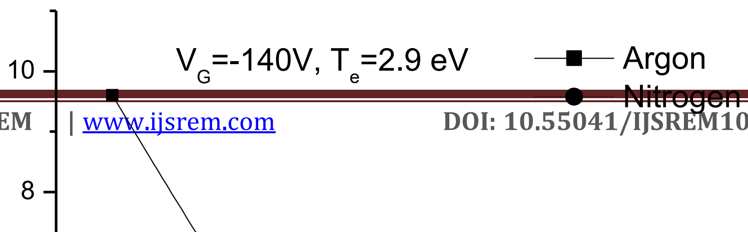
V_G=-140V, T_e=2.9 eV
Argon
Nitrogen

Fig.7